



HAL
open science

Study of the flame propagation from a deck slab to wooden cladding at the laboratory scale

Lucas Terrei, Guillaume Gerandi, Virginie Tihay-Felicelli, Jean-Valère Lorenzetti, Frédéric Morandini, Paul-Antoine Santoni

► **To cite this version:**

Lucas Terrei, Guillaume Gerandi, Virginie Tihay-Felicelli, Jean-Valère Lorenzetti, Frédéric Morandini, et al.. Study of the flame propagation from a deck slab to wooden cladding at the laboratory scale. International Journal of Thermal Sciences, 2024, 195, pp.108664. 10.1016/j.ijthermalsci.2023.108664 . hal-04454634

HAL Id: hal-04454634

<https://hal.science/hal-04454634>

Submitted on 13 Feb 2024

HAL is a multi-disciplinary open access archive for the deposit and dissemination of scientific research documents, whether they are published or not. The documents may come from teaching and research institutions in France or abroad, or from public or private research centers.

L'archive ouverte pluridisciplinaire **HAL**, est destinée au dépôt et à la diffusion de documents scientifiques de niveau recherche, publiés ou non, émanant des établissements d'enseignement et de recherche français ou étrangers, des laboratoires publics ou privés.

Study of the flame propagation from a deck slab to wooden cladding at the laboratory scale

Lucas TERREI^{a,b}, Guillaume GERANDI^{a,c}, Virginie TIHAY-FELICELLI^a, Jean-Valère LORENZETTI^a, Frédéric MORANDINI^a, Paul-Antoine SANTONI^a

^a*CNRS UMR 6134 SPE, University of Corsica, Corte, France*

^b*Université de Lorraine, CNRS, LEMTA, F-54000 Nancy, France*

^c*Laboratoire de Gestion Des Risques Et Environnement UR2334, Université de Haute-Alsace, 68093, Mulhouse Cedex, France*

Abstract

The aim of this work is to improve the understanding of the fire behaviour of building materials used at the wildland urban interface using laboratory scale experiments. To this end, wood cladding was exposed to a propagating flame front across a decking slab. This slab element was ignited by a radiant panel. Three slab configurations were studied: thermoplastic slabs and wooden slabs with slats oriented parallel or perpendicular to the cladding. The vertical distance between the slabs and the cladding varied from 0 to 20 cm and two types of batten arrangement were used to separate the cladding from the supporting cellular concrete. The experiments first focused on the measurement of the heat fluxes received by a non-combustible wall in place of the cladding, depending on the type of slab used. Radiation was the dominant heat flux measured on the wall and it increased up to 35 kW.m⁻² as the flame front approached to the cladding. The spreading of the fire from the slab to the cladding was then investigated. Ignition of the cladding occurred in all configurations tested. The slab configuration (material or orientation) has little effect on the combustion of the cladding once it has been ignited. In addition, the distance between the deck slab and the cladding did not have a significant impact on the fire behaviour of the cladding, even at the 20 cm distance recommended by the standards.

Keywords: WUI fire, wood cladding, fire spread, fire reaction

1. Introduction

Wildland-Urban Interface (WUI) fires are responsible for an increasing number of destroyed structures. The issue of these fires has become a recurring topic around the world [1, 2]. As a result, many studies have been conducted to identify the causes of house fires due to a forest fire [3] and many guidelines [4] have been established such as the minimum water supply, or the vegetation clearing distances around dwellings [5]. On the other hand, regulations on the vulnerability of building materials to forest fires remain weak. In fact, the most detailed standards exist mainly in the United States

18 and Australia, but less so in Europe, where the Mediterranean region is prone to many fires [6, 7].
19 In this region, the probability of building components igniting in a WUI fire is high, but there are no
20 common guidelines for the regulation and layout of the materials involved. Among the materials that
21 can be affected by a forest fire at the Wildland Urban Interface (WUI) (roofing, gutters, windows,
22 doors, terrace,... [8, 9]), the cladding is a key element because it may spread a surface fire to the
23 most vulnerable points of a building such as openings or vents. Many combustible materials are
24 used now in commercial wall assemblies. Moreover, with the enthusiasm for bio-sourced materials,
25 wooden cladding is increasingly present on constructions and can be found on houses located in the
26 WUI.

27
28 Studies of the fire behaviour of cladding vary from the material scale, with cone calorimeter tests
29 [10, 11], to the large scale with a fire escaping from a window of a compartment [12]. Following
30 the Grenfell disaster in 2017, the fire behaviour of facades has become a topic of great interest
31 [13, 14, 15, 16]. However, the fire scenarios often consider a flame exiting from a window hitting the
32 facade. Various standards exist worldwide for testing the fire performance of facades (LEPIR 2, ISO
33 13785-1 [17], DIN 4102-20 [18], BS 8414 series [19], NFPA 285, FM 4880, CAN/ILC-S134). Tests use
34 single walls, corners or walls with windows. Fire can be created either by gas burners or by wood
35 cribs. Nevertheless, whatever the tests, they are far from the conditions that can be encountered
36 during in a WUI fire: the ignition of cladding by direct contact with flames from burning forest fuels,
37 nearby building elements or secondary structures [20, 21], by the radiation [22], or by the projection
38 of firebrands [3, 23].

39 To our knowledge, the only study on wooden walls subjected to an ignition representative of a
40 fire at a WUI is the work of Cohen et al. [24], who studied the ignition of a wooden wall by a crown
41 fire propagating in a jack pine and black spruce forest. The wooden wall of 1.2 m \times 1.2 m with
42 a roof was placed at 10, 20 and 30 m from the burning area. Heat fluxmeters and thermocouples
43 were placed on the wall to assess the impact of the fire. In these experiments, Cohen et al. ob-
44 served that the walls were sometimes ignited but the fire was not sustained and flameout occurred
45 when the vegetation fire had passed the structure. They also showed that some elements can reduce
46 the radiation received by a structure, such as the presence of trees or the fluctuation of the flame front.

47
48 The propagation of a WUI fire to a building can be due to the propagation of the flame front from
49 the vegetation to a building element via combustible material in the vicinity of the constructions
50 [25]. In this work, the fire behaviour of a wooden cladding exposed to a fire front from the burning
51 decks is studied experimentally on a laboratory scale. After quantifying the heat flux received by the

52 cladding during the propagation of the flame front on the decking slab, experiments were performed
53 using a Large Scale Heat Release (LSHR) calorimeter to determine the influence of the decking slab
54 (material, orientation and vertical distance) on the vulnerability of the wooden cladding. The aim of
55 this article is twofold. Firstly, the fire behaviour of wooden cladding exposed to a fire front coming
56 from the burning of decking slabs is studied experimentally to see whether the type of slabs (wood
57 or thermoplastic) influences the vulnerability of the facade. The influence of the vertical distance
58 between the cladding and the decking slabs on the spread of the flame front is then investigated.
59 In many countries, it is indeed recommended to leave a siding clearance between the cladding and
60 the ground to prevent damage from insects and pests. However, this vertical distance varies from
61 country to country and is a key parameter for the spread of a surface fire towards the building.
62 The approach therefore had to follow several stages. First, the fire behaviour of the cladding was
63 studied using a cone calorimeter to obtain reference data (ignition time as a function of flux, Heat
64 Release Rate (HRR), Mass Loss Rate (MLR)). The combustion of the two types of decking slabs
65 was then studied using an LSHR apparatus to measure the HRR of the decking slabs and the heat
66 flux received by a vertical surface placed at their end. Finally, the fire behaviour of wooden cladding
67 ignited by decking slabs was studied, focusing on two parameters that could affect the vulnerability
68 of the cladding, namely the arrangement of the fixing battens and the vertical distance between the
69 bottom of the cladding and the decking slabs. The article first describes the materials and methods
70 used for the experiments. The results are then presented and discussed.

71 **2. Materials and methods**

72 *2.1. Materials*

73 The aim of this work is to study the fire reaction of wooden cladding following the ignition of a
74 decking slab. To this end, two types of decking slabs, thermoplastic and wood, are studied. The fire
75 behaviour of these decking slabs was investigated in previous works [26, 27]. For both materials, the
76 decking slabs measure $40 \times 40 \text{ cm}^2$ with a thickness height of 2.4 cm for the wooden slabs and 5.3 cm
77 for the thermoplastic slabs. More details about the slabs can be found in the work of Tihay-Felicelli
78 et al. [26], such as their thermal properties or ultimate analysis. The wooden slabs, made of pine,
79 are composed of a succession of 6 cm slats spaced 2.5 cm apart and have a weight of $862 \pm 47 \text{ g}$.
80 The thermoplastic slabs are made up of 16 squares of 8.5 cm arranged in four rows and weigh 1597
81 $\pm 21 \text{ g}$.

82 *2.2. Experimental setup at material scale*

83 In order to characterise the fire behaviour of wood cladding, cone calorimeter tests are carried
84 out according to the norm ISO 5660 in vertical orientation. The samples are taken from the cladding
85 boards and are cut to a size of $10 \times 10 \text{ cm}^2$. Prior to the tests, the wood samples are oven dried at
86 $105 \text{ }^\circ\text{C}$ for 24 hours in order to remove any remaining moisture according to the European Norm NF
87 EN ISO 18134. This method of drying did not impact the pyrolysis of wood. For each test, samples
88 are wrapped in a double layer of aluminium and placed in a steel sample holder. The rear side is
89 insulated with a ceramic foam and then a ceramic plate, all held in place by the locking system.
90 The distance between the sample and the cone is fixed at 25 mm as specified by the standard. Each
91 averaged result presented is made up of at least four tests. The experiments last between 15 and 20
92 minutes with imposed heat fluxes ranging from 15 to $45 \text{ kW}\cdot\text{m}^{-2}$ and a piloted spark pilot placed at
93 the center of the exposed surface.

94 *2.3. Experimental setup at product scale*

95 For the need of these experiments, the wood cladding is fixed on cellular concrete with 28 mm
96 thick pine battens. In order to have the highest fluxes at the level of the cladding and therefore to
97 be in the most penalizing configuration, a single decking slab is placed in front of the cladding to
98 have an almost flat flame front [26] and thus avoid a parabolic front. The cladding is cut to obtain
99 a section of $52 \times 50 \text{ cm}^2$, i.e. four boards stacked vertically at a height of 52 cm. This cladding width
100 prevents the flames from passing directly through the side of the cladding towards the rear. Fig. 1
101 shows the detailed configuration of the cladding.

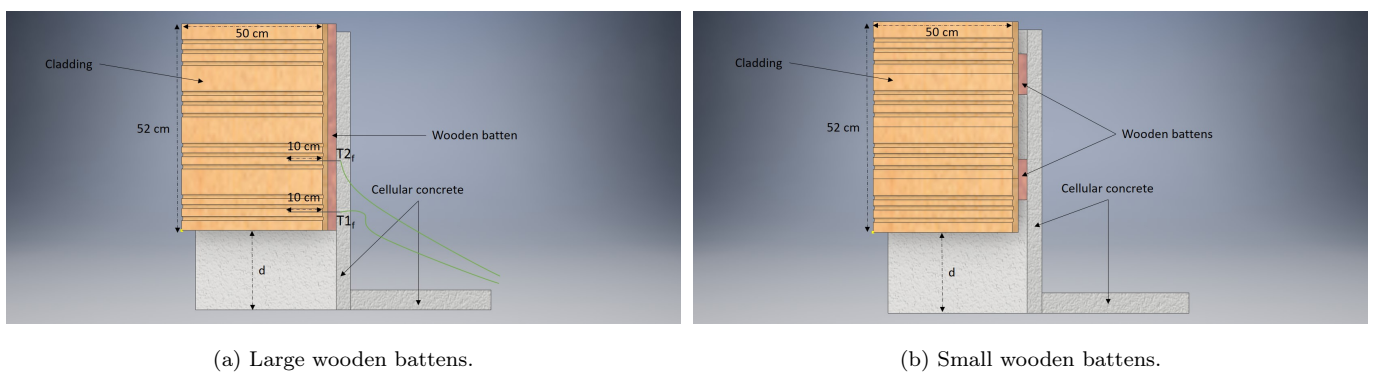
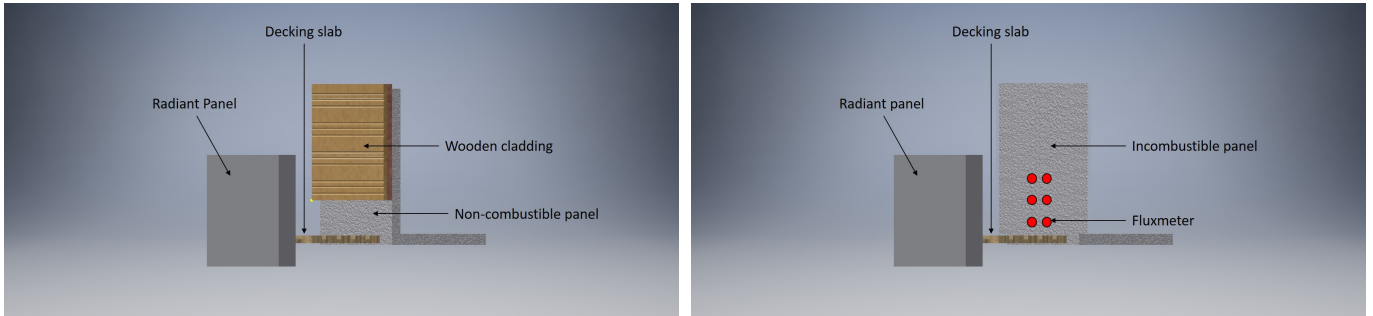


Figure 1: Comparison of the arrangement of the battens that are placed between the cladding and the aerated concrete that will be exposed to the flame front.

102 Two battens configurations are considered. The first, shown in Fig. 1a, involves fixing the battens
103 along the entire length of the cladding. The cladding/batten assembly has a mass of approximately
104 2.3 kg. The second, shown in Fig. 1b, consists of fixing the battens between two boards to attach them

105 at the top and bottom and to hold the structure together, resulting in a total mass of approximately
 106 2.1 kg. The objective of both configurations is to study the effect of the air entrained when the
 107 flame passes between the wood and the cellular concrete. Before each test, the wooden decking slabs,
 108 battens and cladding are oven-dried for 24 hours at 60 °C to reduce the moisture content.

109 The experimental setup is located under the hood of a 1 MW Large Scale Heat Release (LSHR)
 110 apparatus. The fire spreading tests are carried out on a combustion bench covered with cellular
 111 concrete (Fig. 2).



(a) Experimental setup used for the study of fire behavior of the cladding. (b) Experimental setup used for the study of the heat flux received by the non-combustible panel.

Figure 2: Schemes of the experimental setup at product scale.

112 Ignition of the decking slab is provided by a $50 \times 50 \text{ cm}^2$ radiant panel placed 14 cm away from
 113 the edge of the slab. The radiant panel is supplied with propane at a flow rate set to give a constant
 114 heat flux of 35 kW.m^{-2} (measured with a total heat flux gauge) at the leading edge of the slab
 115 exposed to the panel. An electric igniter is positioned 3 cm above this edge to pilot the ignition.
 116 The decking slab is placed against the cladding and the trailing edge of the slab is in contact with
 117 the concrete. The distance between the radiant panel and the wooden cladding is therefore 64 cm.
 118 Different vertical distances between the decking slab and the cladding, noted d (Fig. 1a), are studied:
 119 2, 10 and 20 cm, in order to observe the effect of the height between both elements on the spread of
 120 the flame. The study has been limited to 20 cm because it is the highest value encountered in the
 121 clearance recommendations (used to prevent damage from insects and pests) [28]. As a result, the
 122 cladding was not uniformly exposed to the radiant flux from the panel at the start of the experiment,
 123 but measurements showed that this heat flux, at this distance of 64 cm, did not cause any degradation
 124 of the wood for the time it was in operation. A load cell, with an accuracy of $\pm 3 \text{ g}$ (maximum mass
 125 of 200 kg) and a sampling frequency of 1 Hz, is placed under the combustion bench in order to
 126 measure the mass loss over time. Smoke released during combustion is extracted from the laboratory
 127 by a $1 \text{ m}^3.\text{s}^{-1}$ smoke extraction system and the Heat Release Rate (HRR) is measured by oxygen
 128 consumption. Four K-type thermocouples are stapled to the cladding. Two are placed on the front,

129 at 6.5 cm ($T1_f$) and 18.5 cm ($T2_f$) from the bottom of the cladding and 10 cm from the side (Fig.1a).
130 Two more thermocouples are placed in the same position on the rear side: $T1_b$ at 6.5 cm height and
131 $T2_b$ at 18.5 cm height. Grooves are made on the surface of the wood to match the diameter of the
132 thermocouple (1 mm) so that they can be placed and stapled in place, ensuring contact between the
133 tip of the thermocouple and the wood.

134 According to Tihay-Felicelli et al. [26], the orientation of the wooden decking slab relative to the
135 ignition source can lead to different flame spread and is therefore studied in this work. For the
136 parallel configuration, the slats are oriented parallel to the radiant panel and the cladding, whereas
137 for the perpendicular configuration, they are oriented perpendicular. Fig. A.15 in appendix shows
138 two pictures of the experimental setup with different wooden slabs orientation.

139 Before that, a first set of experiments is carried out to measure the heat flux received by the
140 cladding during the burning of the decking slab. For these experiments, the wooden cladding is
141 replaced by a non-combustible plate (Fig. 2.b), which is drilled along the vertical axis of symmetry,
142 corresponding to the center of the cladding, at different heights (from 2 cm to 42 cm above the slab).
143 Total heat flux gauges (MEDTHERM 64-10-20T, range [0-200] kW.m⁻²) are inserted in these holes
144 to measure the heat flux received by the plate.

145 Twenty-six tests have been carried out to investigate the fire behaviour of the cladding (Fig. 2.a).
146 Three tests per decking slab material have been performed to measure the heat flux received by
147 the cladding. The radiant panel and igniter are lit until the decking slab ignites. Once ignited,
148 they are extinguished to allow the flame to spread across the decking slab in a self-sustaining way.
149 Throughout this article, the time $t=0$ s corresponds to the moment when the decking slabs ignite.
150 This method allows to overcome the differences in the ignition times of the different slabs highlighted
151 by Tihay-Felicelli et al. [26].

152 3. Results and discussion

153 This section first presents the results of the fire behaviour of the wooden cladding at the material
154 scale performed with the cone calorimeter, followed by the results at the product scale carried out
155 with the LSHR apparatus.

156 3.1. Results at material scale

157 For each test, the presence of the spark igniter allows for the ignition of the samples. Fig. 3
158 presents the times-to-ignition according to the heat flux applied.

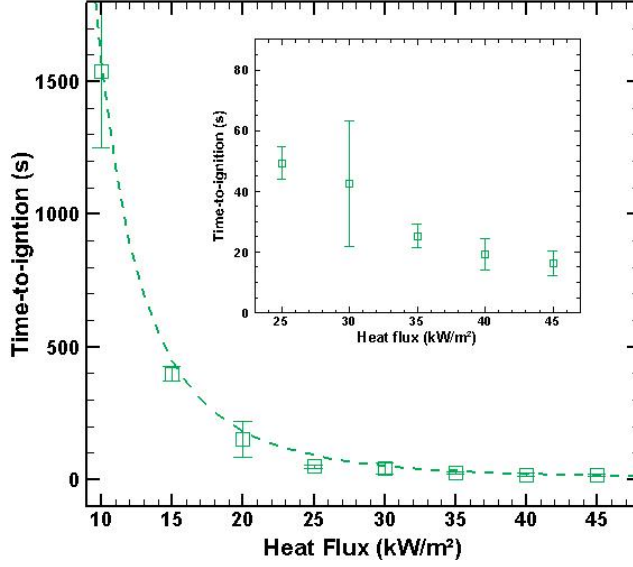


Figure 3: Times-to-ignition as a function of the imposed heat flux.

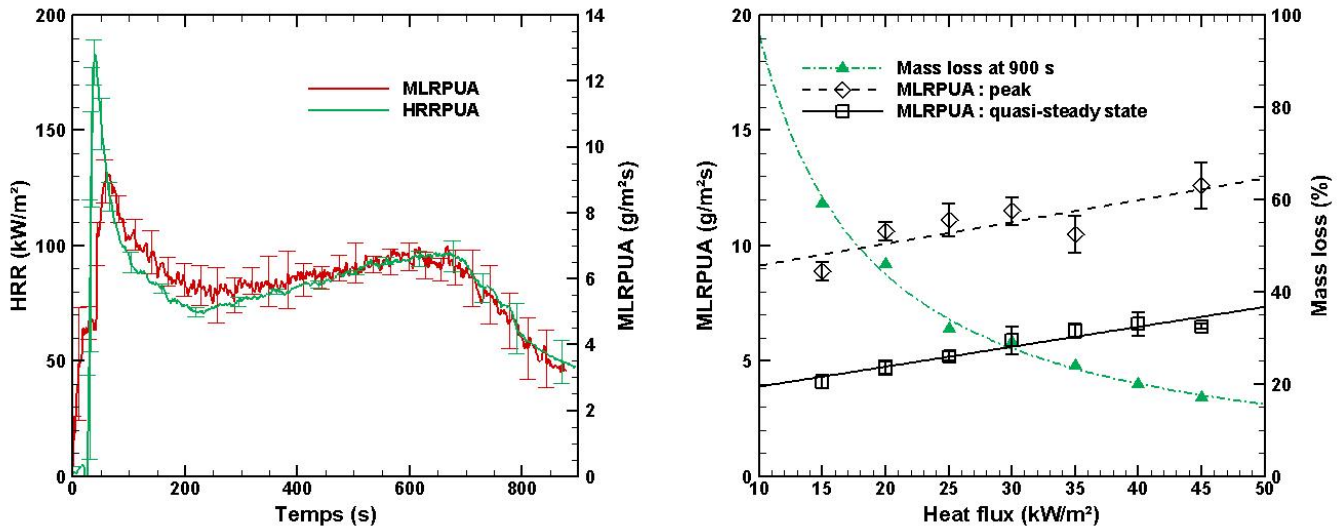
159 Ignition time decreases with increasing heat flux. The repeatability of the results varies with t_{ig}
 160 the applied heat flux and tends to show greater variability when close to the critical heat flux. The
 161 experimental points follow a power law.

162 Based on the ignition times, the Flux-Time Product (FTP) of the wooden cladding is calculated.
 163 The FTP was initially defined by Smith and Satija [29] and is used to estimate the time required
 164 for a combustible material to ignite when exposed to incident radiation [30, 31, 32, 33]. The FTP is
 165 given by the following equation:

$$FTP = t_{ig} \cdot (\dot{q} - \dot{q}_{cr})^n \quad (1)$$

166 where t_{ig} is the time to ignition, \dot{q} is the incident heat flux, \dot{q}_{cr} is the critical heat flux and n is
 167 the power law index.

168 The FTP and the power law index n for the cladding are determined by optimisation (least squares
 169 method) by using the time to ignition data according to the incident heat flux. The calculated FTP
 170 is equal to $4306 \text{ kW}\cdot\text{s}^{1.58}\cdot\text{m}^{-2}$. This result with the exponent $n = 1.58$ is consistent with the values
 171 found in literature [32, 33]. Figures 4a and 4b show the evolutions of the average HRR and MLRPUA
 172 of the tests performed at $35 \text{ kW}\cdot\text{m}^{-2}$ and the mass loss and MLRPUA as a function of heat flux.



(a) Mean MLRPUA and HRRPUA evolutions for 35 kW.m⁻² heat flux. (b) MLRPUA (peak and quasi-steady state) and mass loss as a function of heat flux.

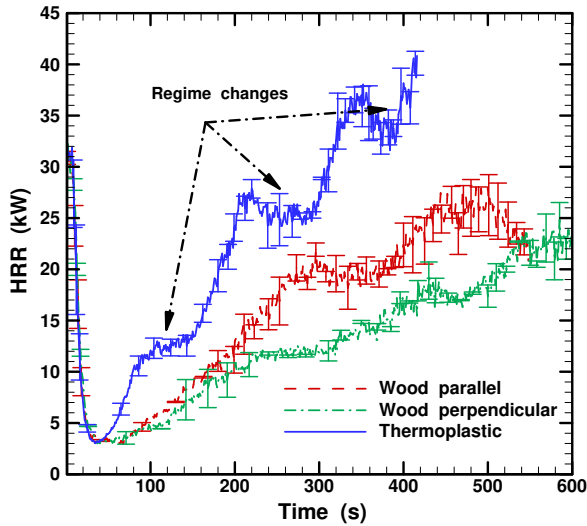
Figure 4: HRRPUA and MLRPUA measured according to the imposed heat flux during the cone experiments.

At 35 kW.m⁻², the exposure of virgin wood to the heat flux results in high degradation and rapid ignition due to the high release of pyrolysis gases and the presence of the pilot. The MLRPUA and HRRPUA increase to a peak. Subsequently, the formation of char on the surface causes the MLRPUA and HRRPUA to decrease to a quasi-stationary phase. During the first 100 seconds, a variation of the MLRPUA and the HRR is observed between the experiments. This stage corresponds to a transient state for which the thickness of the pyrolysis zone could vary from test to test and accentuated by the vertical configuration adopted for the experiments. Subsequently, the formation of char on the surface causes the MLRPUA and HRRPUA to decrease to a quasi-stationary phase, for which the experimental variation does not exceed 10 %. Finally, after 500 s, the degradation of the back side of the wood accelerates again, resulting in a second peak that is smaller than the first one. The peak and the quasi-steady MLRPUA increase quasi-stationary with the applied heat flux, while the mass loss after 900 s of test decreases as a power law. The HRRPUA peak also increases also quasi-linearly with values between 135 and 200 kW.m⁻² for heat fluxes between 15 and 45 kW.m⁻². The results obtained on the wooden cladding with the cone calorimeter allowed to collect data on the ignition time and the HRR as a function of the heat flux and to calculate the FTP of the cladding. These data will be used as a reference to discuss the results obtained at the product scale.

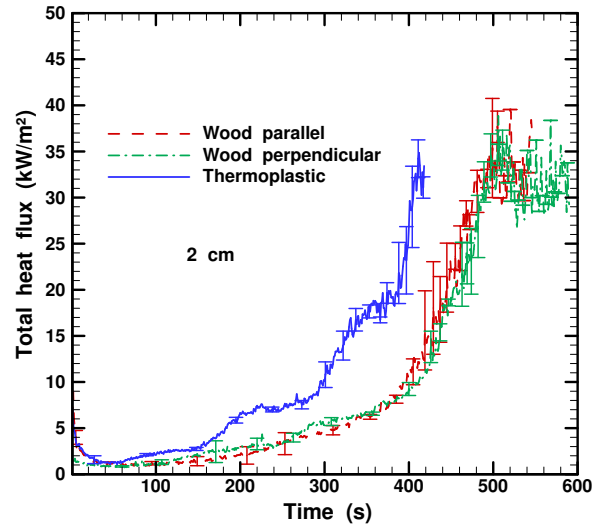
190 3.2. Results at product scale

191 3.2.1. Decking slab combustion and heat flux received by the cladding

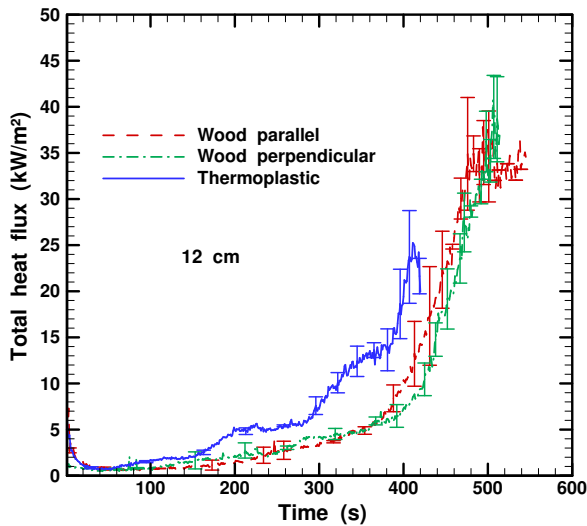
192 Fig. 5 presents the mean Heat Release Rates (HRR) and total heat flux measured received by
193 the heat gauges at the different heights on the non-combustible plate according to the decking slabs
194 studied. At the beginning of the tests, the total heat flux received by the non-combustible plate
195 is between 7 and 9 kW.m⁻². This heat flux is mainly due to the radiant panel. The decrease of
196 the curves at t=10 s corresponds to the extinction of the radiant panel. Immediately after the slab
197 ignition, the HRR released by the burning slabs is only 4 kW, resulting in a total heat flux on the
198 non-combustible plate of about 1 kW.m⁻². As the fire front spreads across the slab towards the non-
199 combustible plate, the HRR increases regardless of the slab's material or configuration. However, the
200 behaviour changes depending on the slab considered. The HRR of the thermoplastic slab is higher
201 and increases faster than that of the wooden slabs. These measurements are consistent with the
202 work of Tihay-Felicelli et al. [26]. Three regime changes are observable on the thermoplastic HRR
203 curves, reflecting the spread of the flame to each new row. The first row produces a HRR of 12 kW
204 (Fig. 5a) and a total heat flux between 1 and 3 kW.m⁻². The HRR then increases to 25 kW with
205 a total heat flux around 7 kW.m⁻². The propagation of the flame front to the third row leads to a
206 HRR around 35 kW and a total heat flux between 12 and 19 kW.m⁻². Finally, the total heat flux
207 increases up to 35 kW.m⁻² at the end of the test, when the flames come into contact with the non-
208 combustible plate. The heat flux measured for the thermoplastic slabs is lower in Fig. 5.b because
209 the experiments have been stopped before the flame came into contact with the non-combustible wall.
210 As highlighted by Tihay-Felicelli et al. [26], the orientation of the wooden decking slab influences
211 the fire behaviour, especially after 200 s. The HRR increase is faster for the parallel configuration
212 than for the perpendicular one. However, the heat fluxes measured on the non-combustible plate are
213 close whatever the orientation considered. After 500 s, the total heat flux ranges between 21 and 45
214 kW.m⁻² depending on the height of the heat flux gauge.



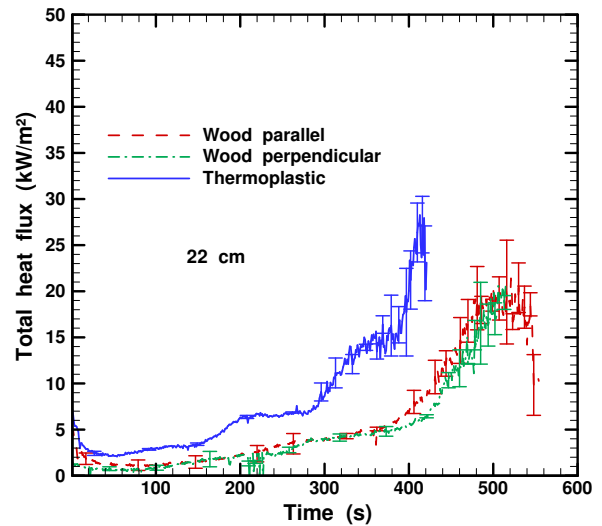
(a) HRR.



(b) Total heat flux at 2 cm height.



(c) Total heat flux at 12 cm height.



(d) Total heat flux at 22 cm height.

Figure 5: Comparison of total heat fluxes received on the non-combustible panel and HRR for the three types of decking slabs.

215 To better visualise the flux distribution on the non-combustible plate, Fig. 6 shows as an example
 216 a mapping of the mean total heat fluxes obtained from the measurements at 2, 12, 22 and 32 cm
 217 for the experiments with the thermoplastic slab. Up to 300 s for the wooden slabs and 200 s for
 218 the thermoplastic slabs, the heat fluxes are almost constant over each height of the non-combustible
 219 plate. The heat flux received at a height of about 2 cm is the highest. Above that, the recorded values
 220 are very close. As the fire front propagates through the slab, the base of the flame is indeed thicker
 221 generating more radiation at the lower part of the plate. As the fire front propagates through the
 222 slab, the shape of the fire front takes on a triangular shape [26]. The base of the flame is thus thicker

223 generating more radiation at the lower part of the plate. From 400 s, the heat flux increases strongly
 224 because the flame front is very close to the fluxmeter and can reaches the sensors. Despite the fact
 225 that the flame front coming from the decking slabs is quasi-straight, the heat flux should decrease
 226 slightly away from the center, as the view factor also decreases due to the boundary conditions of
 227 the experiments.

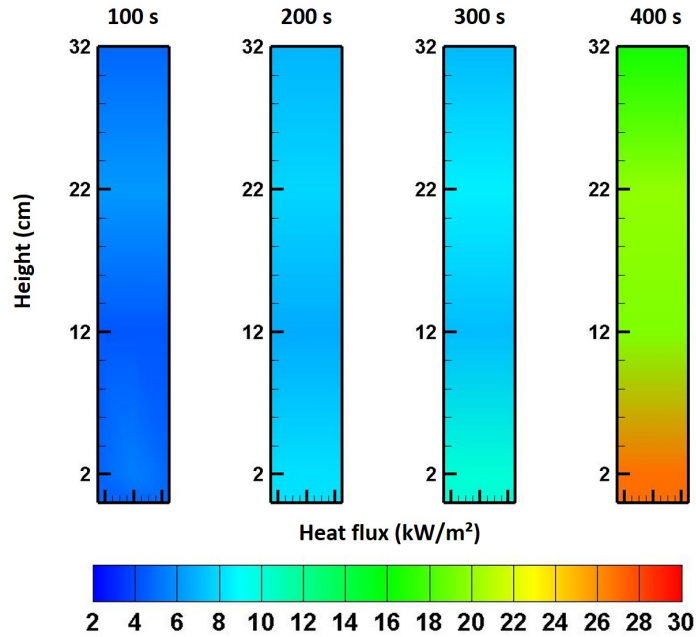
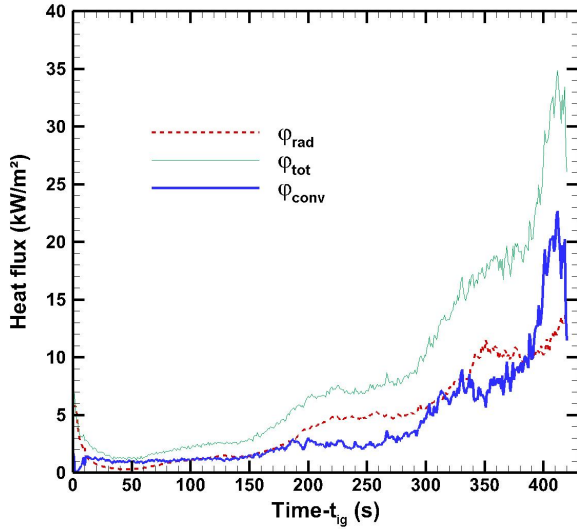
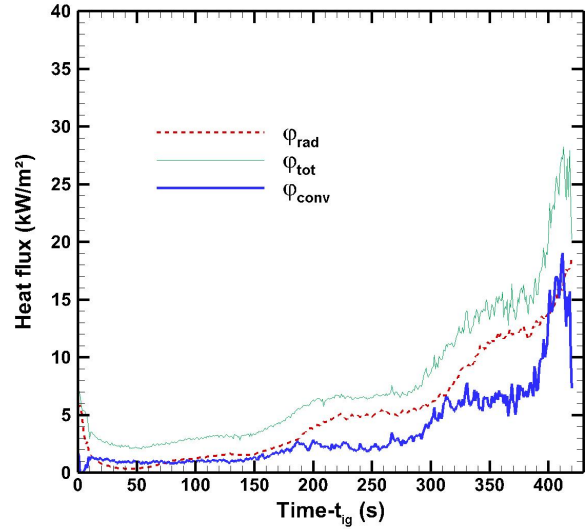


Figure 6: Mapping of mean total heat fluxes measured at 100, 200, 300 and 400 seconds during the experiments with thermoplastic slab and non-combustible plate.

228 The contribution of radiant and convective heat fluxes during fire propagation on the decking
 229 slabs have [has](#) been evaluated on the non-combustible plate. This has been done by replacing the
 230 total heat flux gauges with radiant gauges in three additional tests with thermoplastic decking slabs.
 231 The presence of a convective heat flux (φ_{conv}) is assessed from the radiant heat flux (φ_{rad}) and the
 232 total heat flux (φ_{tot}) using the following equation: $\varphi_{conv} = \varphi_{tot} - \varphi_{rad}$. Fig. 7 presents the evolution
 233 of the different heat fluxes for two heights after the ignition of the thermoplastic decking slab. From
 234 0 to 150 s, the convective and radiant heat fluxes are close, between 1 and 2 kW.m⁻². From 175 s,
 235 the radiation is the dominant heat transfer measured at 5 kW.m⁻². The cladding will not degrade
 236 or ignite at this heat flux value. After 300 s, the flame front approaches the non-combustible plate.
 237 The fluctuations increase due to the intensification of the convective part. The radiation is the
 238 predominant heat transfer except at 2 cm. At this height, the convection becomes higher when the
 239 flame front reaches the non-combustible plate.



(a) 2 cm.



(b) 22 cm.

Figure 7: Evolution of total, radiant and convective heat fluxes for two heights during the burning of a thermoplastic decking slab.

240 Studying the combustion of the decking only has allowed us to measure the heat release rate of
 241 the decking slabs as well as the heat flux received on a vertical surface placed at their end. It has been
 242 shown that the flame front propagates with different dynamics depending on the type of decking slab
 243 and also on the orientation of the wooden slats. The flux received by the vertical non-combustible
 244 panel increases as the flame front approaches, reaching values higher than $35 \text{ kW}\cdot\text{m}^{-2}$ when the flame
 245 front comes into contact with the fluxmeters. The orientation of the slats of the wooden panel does
 246 not appear to affect the heat flux received by the vertical panel.

247 3.2.2. Fire behaviour of the cladding

248 Fig. 8 shows a typical fire spread test over time, from the ignition of the slab to the extinction
 249 of the cladding. The arrangement of the wooden battens was with the small one (Fig. 1b).

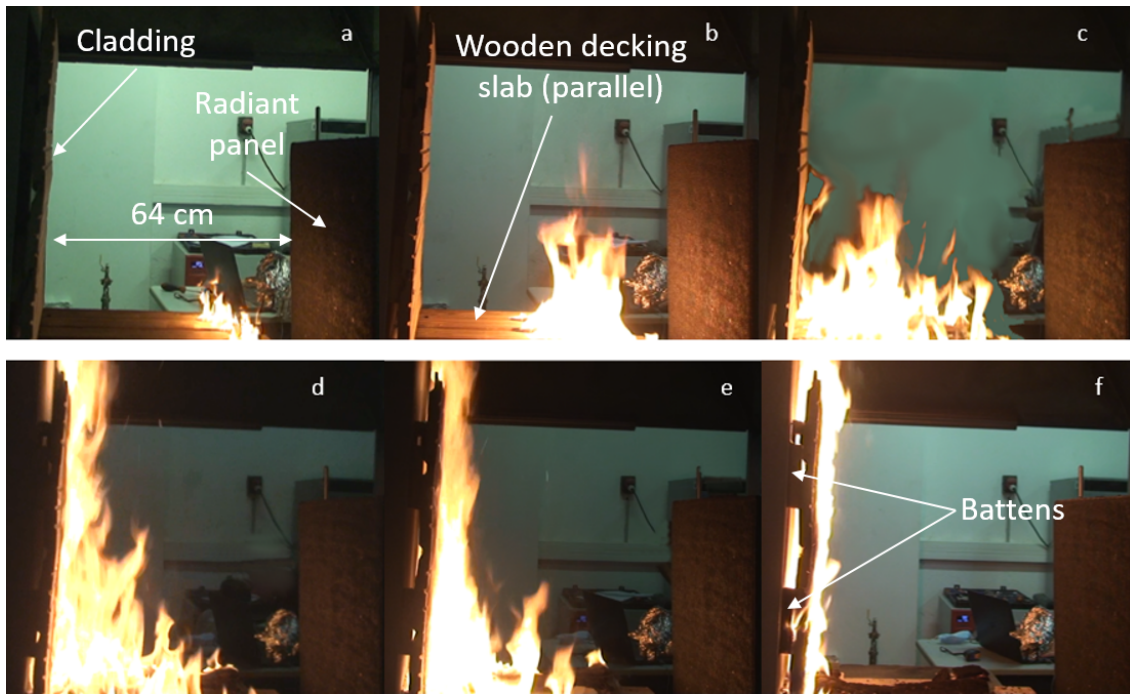


Figure 8: Photographs of a experiment performed with a wooden decking slab in perpendicular configuration and small wooden battens a) Ignition of the decking slab (t=0 s) b) Propagation of the flame front on the slab (t=210 s) c) Ignition of the wooden cladding (t=430 s) d) Propagation of the flame front on the cladding (t=480 s) e) Ignition of the rear face of the cladding (t=550 s) f) Extinction phase (t=840 s).

250 Fig. 8.a shows the decking slab just ignited by the radiant panel (here turned off). Ignition occurs
 251 at the leading edge of the first slat of the slab exposed to the panel due to the ignition of pyrolysis
 252 gases by the igniter. The flame front then spreads across the entire width of the slab and advances
 253 towards the cladding (Fig. 8.b). The wooden cladding is ignited on its lower part by direct contact
 254 with the fire front (Fig. 8.c). Although the heat fluxes received by the wooden cladding may exceed
 255 $25 \text{ kW}\cdot\text{m}^{-2}$ before the flame front reaches it (Fig. 5), it is not sufficient to ignite it without flame
 256 contact. This is consistent with the results obtained with the cone calorimeter. Indeed, considering
 257 the highest fluxes measured on the non-combustible panel, i.e. at a height of 2 cm of the cladding
 258 (Fig. 5), before the flame front reaches the end of the decking slabs, the flux received by the verti-
 259 cal panel exceeds $25 \text{ kW}\cdot\text{m}^{-2}$ only between 21 and 36 s and $30 \text{ kW}\cdot\text{m}^{-2}$ only between 10 and 23 s,
 260 depending on the decking slabs. These times are much lower than the ignition times measured with
 261 the cone calorimeter for these heat fluxes. Once the cladding has ignited, the flame spread over the
 262 surface exposed to the fire is very fast resulting in its generalized combustion (Fig. 8.d) with ignition
 263 of the rear face (Fig. 8.e). When all the virgin wood on the decking slab surface has turned into char,
 264 the flame intensity decreases but the wood continues to degrade until it is completely transformed
 265 into char (Fig. 8.f). After the flameout, a smoldering phase occurs on the parts of the cladding that
 266 have not collapsed or been completely consumed by the fire.

268 Fig. 9 shows the HRR and normalised mass loss for wooden cladding located 20 cm above a
269 thermoplastic decking slab. These curves concern the whole test, from the ignition of the decking
270 slab to the extinction of the cladding. The HRR measured before $t=0$ s corresponds to the radiant
271 panel HRR. The panel is switched off at $t=0$ s when the decking slab ignites. The mass starts to
272 decrease from the beginning of the experiment as it is measured for both the cladding and the decking
273 slab, the latter degrading as a result of its exposure to the radiant panel. The experiment is divided
274 into four stages. The first phase corresponds to the spread of the flame front over the 40 cm of the
275 decking slab (Region A). This zone is similar in intensity and duration to the results presented for
276 the combustion of the thermoplastic slab (Fig. 5). The mass loss is mainly due to the combustion of
277 the decking slab. After the ignition of the wooden cladding (Region B), the mass decreases sharply
278 and the HRR increases very rapidly to reach a first peak. During this phase, the measured mass
279 loss and the HRR are mainly due to the cladding burning, although some is due to the end of the
280 decking slab combustion. A second peak of HRR then occurs at 680 s (Region C), due to the whole
281 burning of the cladding, including its rear face. In fact, the separation caused by the wooden battens
282 between the cellular concrete allows the flame to engulf through this air gap, further intensifying the
283 heat released by the fire. [This phenomenon can only be observed at the product scale and shows](#)
284 [the interest of studying the fire behavior of the cladding at this scale.](#) After the flameout (Region
285 D), the mass continues to decrease slowly due to the smoldering until the complete extinction. The
286 burning time of the cladding is about 700 s, close to the degradation of the cladding sample at the
287 material scale for an imposed heat flux of $35 \text{ kW}\cdot\text{m}^{-2}$. Indeed, Fig. 4 shows that the HRR and MLR
288 at the cone calorimeter decrease rapidly from 700 s onwards, indicating that the virgin wood is fully
289 burnt from this moment.

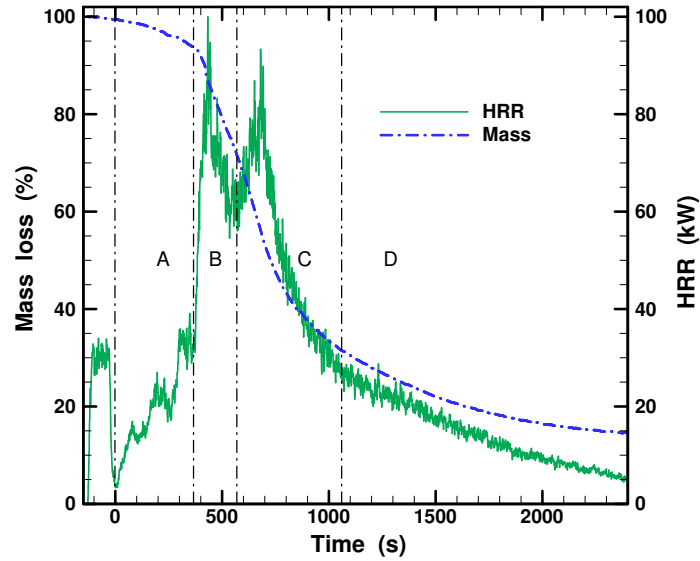


Figure 9: HRR and normalised mass loss of a cladding test located at 20 cm height above a thermoplastic slab. Region A: flame front spreading over the decking slab, Region B: ignition of the wooden cladding, Region C: total combustion of the wooden cladding, Region D: flameout.

290 Fig. 10 shows the temperatures on the front and rear sides of the cladding at 6.5 and 18.5 cm
 291 height for an experiment with a thermoplastic slab ($d = 20$ cm). The HRR is added to facilitate
 292 the discussion of the results. Temperatures cannot be measured throughout the test because the
 293 detachment of the sensor from the cladding surface during the degradation of the wood causes
 294 significant fluctuations in the measurements. As the fire spreads across the deck slab, the temperature
 295 of the front of the wooden cladding slowly increases. The temperature of the lower part (T_{1f}) of
 296 the cladding increases more rapidly which is consistent with the higher heat fluxes at the base of the
 297 cladding. However, the temperature of the front face of the cladding does not exceed 180 °C until
 298 the flame front is close enough to it. This temperature is not sufficient to allow thermal degradation
 299 of the wooden cladding, which begins around 220 °C, and therefore ignition by radiation. Once the
 300 fire front reaches the end of the slab, the temperature measured on the cladding increases rapidly.
 301 This allows the wood to degrade and ignite. The temperature rise of the rear face is shifted from
 302 that of the front face. As for the exposed face, the temperature is initially higher at the bottom due
 303 to the presence of the flame front. The temperature at the top of the rear face is only high enough
 304 to degrade the wood once the first HRR peak has passed, confirming that the second HRR peak is
 305 due to the complete combustion of both sides of the cladding.

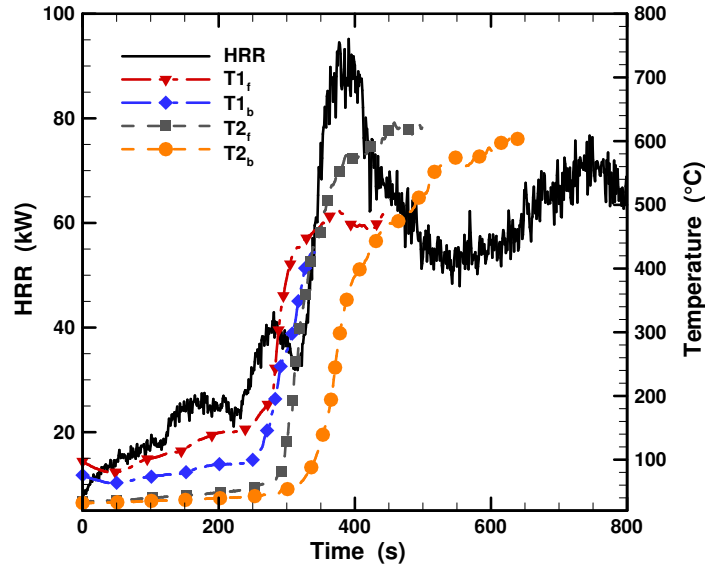


Figure 10: HRR and temperatures on the front and back sides of the wooden cladding for an experiment with a thermoplastic decking slab.

306 There are many ways to study the ignition of materials, such as ignition temperature, critical
 307 mass flux or FTP. In this study, the FTP was tested because this method was used by Cohen et
 308 al. [24] to determine the ignition of wood cladding in large-scale tests. To investigate whether the
 309 FTP determined at the material scale is an appropriate criterion for predicting the ignition of the
 310 cladding, the FTP over time calculated from the heat fluxes measured on the non-combustible panel
 311 at 2 cm height (Fig. 5) is plotted in Fig. 11. This is performed only for the thermoplastic slab, which
 312 had the highest repeatability. The dotted horizontal line corresponds to the FTP value determined
 313 at the material scale. The HRR of the cladding has been obtained by subtracting the mean total
 314 HRR (thermoplastic slab and wooden cladding) and the HRR measured during experiments with
 315 thermoplastic slabs only. Ignition occurs slightly before the FTP reaches the value corresponding to
 316 the ignition. This is probably due to pilot ignition which is more effective with flame contact than
 317 with the cone calorimeter igniter. Despite this small shift, the FTP appears to give a satisfactory
 318 prediction of cladding ignition. The cone calorimeter appears to be an experimental setup that
 319 enables the piloted ignition of materials to be predicted fairly accurately, but it is necessary to carry
 320 out tests on a product scale in order to understand overall fire behaviour, from ignition to extinction.

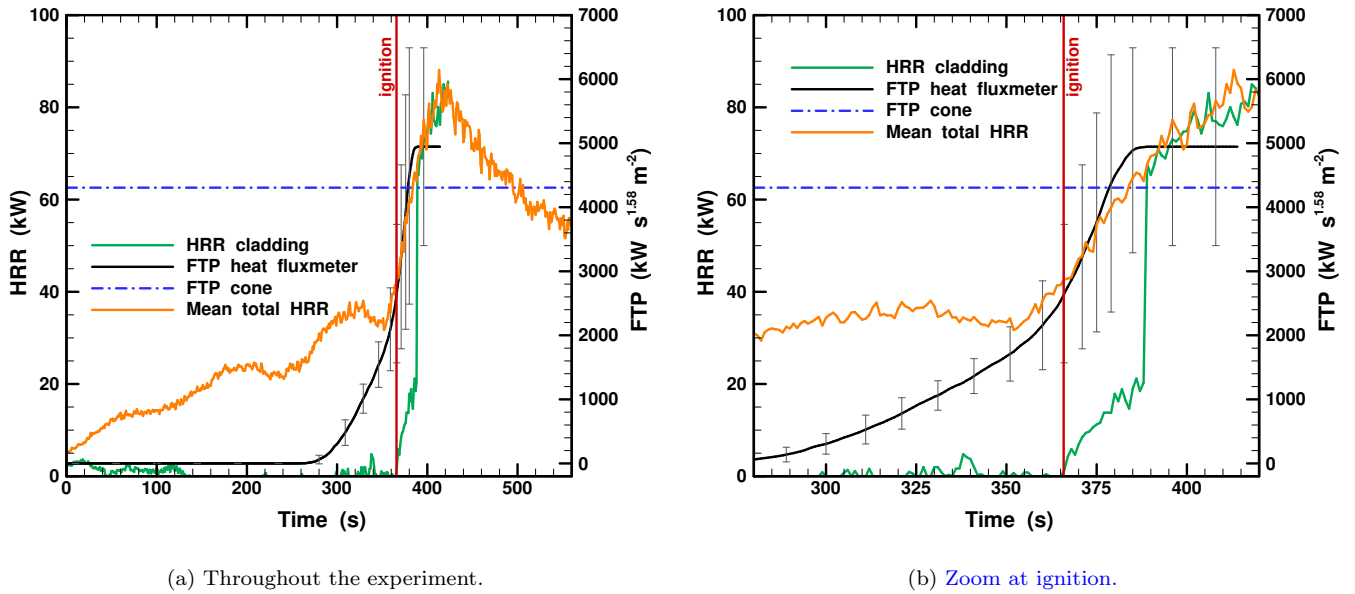


Figure 11: HRR and FTP for an experiment with a thermoplastic slab.

321 In order to compare the fire behaviour of the cladding after its ignition, the average mass loss,
 322 mass loss rate and HRR are plotted in Fig. 12 for the three types of decking slabs. Due to the
 323 greater spread of the flame front, wood cladding has always ignited more quickly with thermoplastic
 324 slabs. In this figure, $t=0$ s corresponds to the ignition of the cladding to facilitate the comparison.
 325 Table 1 summarises the main fire indicators. Regardless of the configuration considered, the MLR
 326 and HRR curves show two peaks, corresponding to the two combustion phases of the cladding. The
 327 first peak occurs at about 100 s after the cladding ignition and the second one at about 400 s. The
 328 evolution of HRR, MLR and mass loss is very similar for both wooden slab configurations, whether
 329 the slab is parallel or perpendicular to the cladding. The two peaks of MLR are between 4.4 and
 330 $5.6 \text{ g}\cdot\text{s}^{-1}$, while the two peaks of HRR are in the range of 51-55 kW. The HRR of the thermoplastic
 331 slabs is higher than that of the wooden slabs throughout the tests. In fact, the first peak of the
 332 HRR reaches an average of 86 kW, while the second peak reaches 65 kW. This increase is due to the
 333 combustion of the thermoplastic slab which releases an HRR of approximately 20 kW higher than
 334 that of the wooden slabs (Fig. 5a). Once ignited, the fire dynamics of the cladding are therefore
 335 little influenced by the ignition source. At the end of the experiments, only ashes remain for the
 336 tests with the wooden decking slab and the cladding. For the tests with the thermoplastic slab, it
 337 remains 0.42 ± 0.06 kg, corresponding mainly to the residue coming from the calcium carbonate used
 338 as a filler in the thermoplastic decking slab.

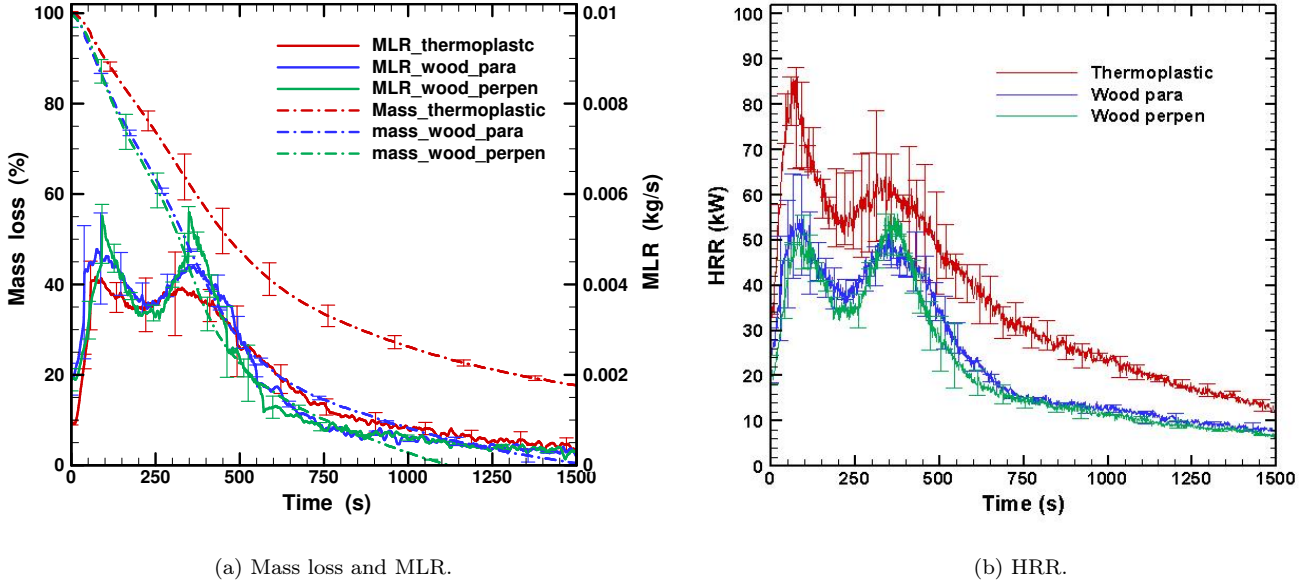


Figure 12: Evolution of MLR, mass loss and HRR of the cladding placed 20 cm high and ignited by the three decking slab types.

Table 1: Mass loss at 600 s, peaks of HRR and MLR for the different decking slabs and and a gap of 20 cm between the slab and the cladding.

Material	Orientation	Mass loss at 600 s (%)	MLR _{peak1} (g.s ⁻¹)	MLR _{peak2} (g.s ⁻¹)	HRR _{peak1} (kW)	HRR _{peak2} (kW)
Thermoplastic		60±3	4.2±0.7	3.9±0.9	86±12	65±20
Wood	Parallel	79±1	4.8±1.0	4.4±0.1	55±11	51±1
	Perpendicular	81 ±1	5.5±1.0	5.6±0.8	51±5	55±1

339 The study of the fire behavior of the cladding has shown that the cladding is ignited at the bottom
340 by direct contact with the flame front coming from the slabs. The heat flux received by the cladding
341 during the propagation of the fire on the slabs does not allow the temperature of the cladding to rise
342 enough to allow ignition by radiation. Once ignited, the combustion dynamics of the cladding is not
343 influenced by the type of decking slabs. Combustion begins on the exposed face and then spreads to
344 the back face, resulting in a generalized burning of the cladding.

345 3.2.3. Effect of the batten arrangement

346 Fig. 13 compares the HRR and the mass loss after the cladding ignition for the long and short
347 battens configurations for a distance of 20 cm between the slab and the cladding. The evolution of
348 the HRR is similar for both battens. The change in size and configuration does not seem to have a

349 significant influence on the overall behaviour of the cladding once it is ignited. The difference in HRR
 350 is a maximum of 7 and 9 kW for the first and second peaks respectively. Otherwise it is between 1
 351 and 5 kW, which is within the standard deviation of the experiments. The evolution of the mass loss
 352 is generally similar, although the mass loss of the long batten configuration decreases more rapidly.
 353 This can be explained by the addition of fuel from the battens themselves, but above all by the
 354 greater chimney effect caused by the presence of the long battens, which favours the combustion of
 355 the wood at the rear face. Thus, the combustion of the cladding is little affected by the size of the
 356 battens. This parameter does not seem to be a key parameter in the fire behavior of the cladding.

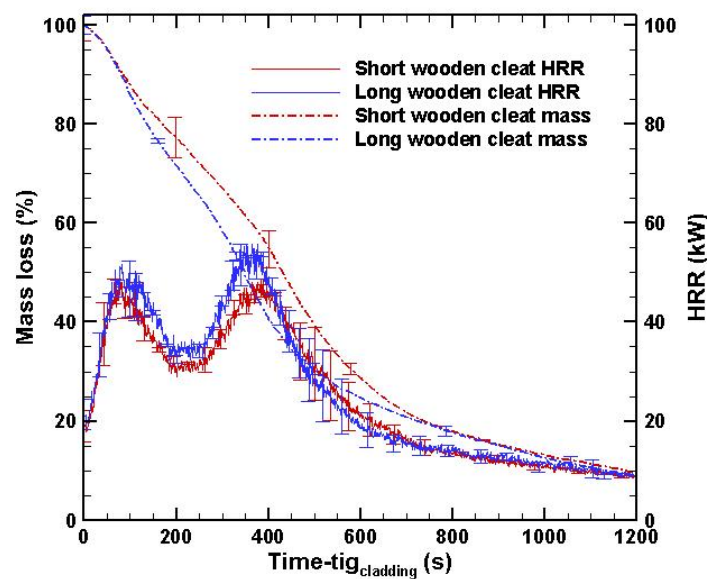


Figure 13: Comparison of HRR and normalised mass losses according to the type of wooden battens.

357 3.2.4. Effect of vertical distance on the fire behaviour of cladding and wooden slabs orientations

358 The influence of the vertical distance between the cladding and the decking slab is only studied
 359 for the wooden decking slabs. Three distances are tested: 20, 10 and 2 cm. In France, the DTU 41.2
 360 standard [28] stipulates that the distance between the ground and the cladding must be equal to
 361 20 cm. However, owners may have to change the layout of their home, in particular by installing a
 362 terrace at a later date. Fig. 14 shows the mean HRR, mass loss and MLR for the different distances
 363 and both orientations of the wooden decking slabs. Table 2 presents the main fire indicators for the
 364 different heights and configurations of wooden slabs.

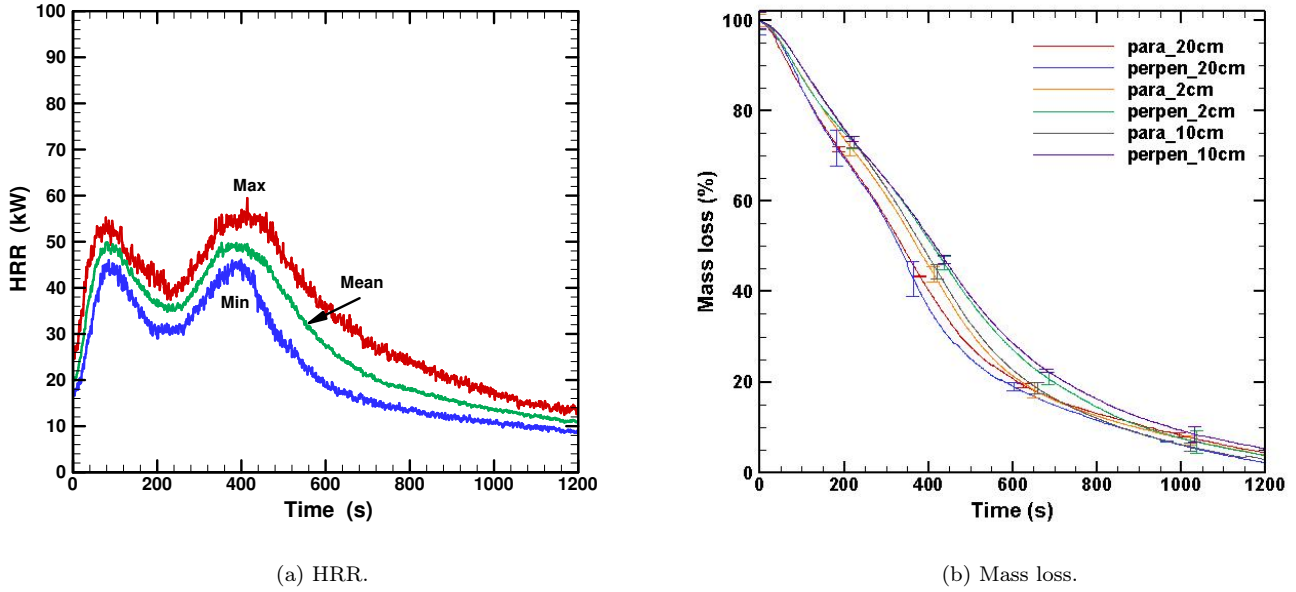


Figure 14: Evolution of HRR and mass losses for the different gaps between cladding and wooden decking slabs (height of 2, 10 and 20 cm).

Table 2: Mass loss at 600 s, peaks of HRR and MLR for the different gaps between cladding and wooden decking slabs.

Orientation	d (cm)	Mass loss at 600 s (%)	MLR_{peak_1} ($g.s^{-1}$)	MLR_{peak_2} ($g.s^{-1}$)	HRR_{peak_1} (kW)	HRR_{peak_2} (kW)
parallel	2	79 ± 2	3.8 ± 0.2	4.1 ± 0.1	52 ± 5	56 ± 3
	10	78 ± 1	3.4 ± 0.2	3.9 ± 0.01	49 ± 5	59 ± 2
	20	79 ± 1	4.8 ± 1.0	4.4 ± 0.1	55 ± 11	51 ± 1
perpendicular	2	73 ± 2	3.7 ± 0.2	3.5 ± 0.3	53 ± 2	50 ± 3
	10	72 ± 1	3.5 ± 0.3	3.4 ± 0.1	52 ± 4	53 ± 6
	20	81 ± 1	5.5 ± 1.0	5.6 ± 0.8	51 ± 5	55 ± 1

365 The tests are slightly more repeatable at a distance of 2 cm compared to 20 cm. This observation
366 is due to the higher heat fluxes received on the lower part of the cladding (Fig. 5), which facilitates
367 a homogeneous ignition of the wooden cladding. With regard to the influence of the decking slab,
368 the spacing between the decking slab and the cladding does not have a significant impact on the
369 fire behaviour of the cladding once it has ignited. Indeed, the evolution of HRR and mass loss is
370 similar for all configurations (Table 2). The mass loss at 600 s varies between 72 and 81 % to reach
371 a residual mass at 1200 s between 2 and 5 %, mainly ashes. The two HRR peaks are between 49 and
372 59 kW with no particular trend observed. The MLRs also have similar peaks between 3.4 and 5.6

373 $\text{g}\cdot\text{s}^{-1}$, with slightly higher peaks for a spacing of 20 cm. This weak influence of the spacing on the
374 fire behaviour of the cladding is probably due to the fact that the flames produced by the wooden
375 decking slabs are approximately 33 cm in length, resulting in direct contact regardless of the spacing
376 tested. Since ignition occurs by direct contact, it would be safer to require an additional horizontal
377 discontinuity between the decking slab and the cladding. Thus, no effect on the vulnerability of the
378 cladding was observed for the distances tested between the decking slabs and the cladding. A vertical
379 distance of 2, 10 or 20 cm always induces ignition of the cladding by the flame front resulting from
380 the combustion of the decking slabs. This weak influence of the spacing on the fire behaviour of the
381 cladding is probably due to the fact that the flames generated by the wooden decking slabs have a
382 length of approximately 33 cm, resulting in direct contact regardless of the spacing tested. Since
383 ignition occurs by direct contact, it would be safer to require an additional horizontal discontinuity
384 between the decking slab and the cladding.

385 4. Conclusion

386 The experimental setup in this study allows the investigation of the propagation of a flame front
387 from a horizontal material used in the exterior of a dwelling (decking slab) to a vertical material such
388 as wooden cladding. The influence of the decking slab material and its orientation as well as the ver-
389 tical distance between the slab and the cladding were investigated. For the three slab configurations
390 tested, the radiant heat flux is the dominant heat transfer mode during the fire propagation on the
391 slab. Ignition of the wooden cladding occurs only by direct contact, as the temperature increase on
392 the cladding is not sufficient to allow an ignition by radiation. The 21 tests performed to study the
393 fire behaviour of the cladding have shown that:

- 394 • Slab configuration has little effect on cladding combustion once it is ignited. There are two
395 peaks in the MLR and HRR. The first one is due to the ignition of the front face of the
396 wooden cladding, whereas the second peak corresponds to the ignition of the back face after
397 the penetration of the flame into the gap separating the cladding from the cellular concrete
398 wall.
- 399 • The vertical spacing (for the range considered in this study, 2 cm to 20 cm) between the decking
400 slab and the cladding does not impact significantly the fire behaviour of the cladding.

401 These tests have shown that in the absence of extreme conditions such as wind, wooden cladding
402 positioned at the end of a combustible decking slab will ignite and burn completely. A vertical spacing
403 of 20 cm (according to the standards) does not prevent the spread of the fire. It therefore seems

404 necessary to recommend an additional horizontal separation, since ignition takes place by direct
405 contact with the flame front. It would also be interesting to recommend the use of an incombustible
406 barrier between the cladding and the wall to avoid the chimney effect and the ignition of the rear
407 face.

408 Appendix A. Appendices



Figure A.15: Orientation of wooden decking slabs for a vertical distance of 2 cm between the cladding and the slab.

409 References

- 410 [1] J. Cohen, “The wildland-urban interface fire problem: A consequence of the fire exclusion
411 paradigm,” Forest History Today. Fall: 20-26., pp. 20–26, 2008.
- 412 [2] S. E. Caton, R. S. Hakes, D. J. Gorham, A. Zhou, and M. J. Gollner, “Review of pathways for
413 building fire spread in the wildland urban interface part i: exposure conditions,” Fire technology,
414 vol. 53, no. 2, pp. 429–473, 2017.
- 415 [3] J. D. Cohen and R. D. Stratton, “Home destruction examination: Grass valley fire, lake arrow-

- 416 head, california,” Tech. Paper R5-TP-026b. Vallejo, CA: US Department of Agriculture, Forest
417 Service, Pacific Southwest Region (Region 5). 26 p., 2008.
- 418 [4] R. H. White, D. DeMars, and M. Bishop, “Flammability of Christmas trees and other vegeta-
419 tion,” in Proceedings of the 24th international conference on fire safety, pp. 21–24, Products
420 Safety Corporation, 1997.
- 421 [5] “NFPA 1144 standard for reducing structure ignition hazards from wildland fire,” 2013.
- 422 [6] A. Ganteaume and M. Jappiot, “What causes large fires in southern France,” Forest Ecology
423 and Management, vol. 294, pp. 76–85, 2013.
- 424 [7] A. Ganteaume, A. Camia, M. Jappiot, J. San-Miguel-Ayanz, M. Long-Fournel, and C. Lampin,
425 “A review of the main driving factors of forest fire ignition over Europe,” Environmental
426 management, vol. 51, no. 3, pp. 651–662, 2013.
- 427 [8] G. Xanthopoulos, “Factors affecting the vulnerability of houses to wildland fire in the Mediter-
428 ranean region,” in Proceedings of the international workshop forest fires in the wildland-urban
429 interface and rural areas in Europe, pp. 15–16, 2003.
- 430 [9] S. L. Manzello, S. Suzuki, and Y. Hayashi, “Enabling the study of structure vulnerabilities to
431 ignition from wind driven firebrand showers: A summary of experimental results,” Fire Safety
432 Journal, vol. 54, pp. 181–196, 2012.
- 433 [10] K. Nguyen, N. K. Kim, D. Bhattacharyya, and A. Mouritz, “Assessing the combustibility of
434 claddings: A comparative study of the modified cone calorimeter method and cylindrical furnace
435 test,” Fire and Materials, 2021.
- 436 [11] M. S. McLaggan, J. P. Hidalgo, J. Carrascal, M. T. Heitzmann, A. F. Osorio, and J. L. Torero,
437 “Flammability trends for a comprehensive array of cladding materials,” Fire safety journal,
438 vol. 120, p. 103133, 2021.
- 439 [12] I. Oleszkiewicz, “Fire exposure to exterior walls and flame spread on combustible cladding,” Fire
440 Technology, vol. 26, no. 4, pp. 357–375, 1990.
- 441 [13] S. T. McKenna, N. Jones, G. Peck, K. Dickens, W. Pawelec, S. Oradei, S. Harris, A. A. Stec,
442 and T. R. Hull, “Fire behaviour of modern façade materials - understanding the grenfell tower
443 fire,” Journal of Hazardous Materials, vol. 368, pp. 115–123, 2019.

- 444 [14] E. Guillaume, T. Fateh, R. Schillinger, R. Chiva, and S. Ukleja, “Study of fire behaviour of facade
445 mock-ups equipped with aluminium composite material-based claddings, using intermediate-
446 scale test method,” Fire and Materials, pp. 1–17, 2018.
- 447 [15] M. Bonner and G. Rei, “Flammability and multi-objective performance of building façades:
448 Towards optimum design,” International Journal of High-Rise Buildings, vol. 7, no. 4, pp. 363–
449 374, 2018.
- 450 [16] P. Cancelliere, P. Canzani, S. Sassi, A. Lucchini, S. Messa, and E. Anselmi, “A new test method
451 to determine the fire behavior of façades with etic system,” Fire and Materials, vol. 45, pp. 624–
452 637, 2021.
- 453 [17] H. Yang et al., “Basic research of fire properties of exterior insulation and finish systems,
454 part3: Reaction-to-fire tests for facades–intermediate-scale test (iso 13785-1),” in Summaries
455 of Technical Papers of Annual Meeting, Architectural Institute of Japan, 2009.
- 456 [18] D. 4102-20, “Fire behaviour of building materials and building components—part 20: Comple-
457 mentary verification for the assessment of the fire behaviour of external wall claddings,” Afnor,
458 2017.
- 459 [19] B. S. I. (BSI), “Bs 8414-1:2020-04 fire performance of external cladding systems part 1: Test
460 method for non- loadbearing external cladding systems fixed to, and supported by, a masonry
461 substrate,” British Standards Institution: London, 2020.
- 462 [20] S. L. Quarles, Y. Valachovic, G. M. Nakamura, G. A. Nader, and M. J. De Lasaux, “Home
463 survival in wildfire-prone areas: building materials and design considerations,” 2010.
- 464 [21] V. Babrauskas, “Ignition handbook-principles and applications to fire safety engineering, fire
465 investigation, risk management and forensic science,” 2003.
- 466 [22] V. Babrauskas and W. J. Parker, “Ignitability measurements with the cone calorimeter,” Fire
467 and materials, vol. 11, no. 1, pp. 31–43, 1987.
- 468 [23] A. Ganteaume, M. Guijarro, M. Jappiot, C. Hernando, C. Lampin-Maillet, P. Pérez-Gorostiaga,
469 and J. A. Vega, “Laboratory characterization of firebrands involved in spot fires,” Annals of
470 Forest Science, vol. 68, no. 3, pp. 531–541, 2011.
- 471 [24] J. D. Cohen, “Relating flame radiation to home ignition using modeling and experimental crown
472 fires,” Canadian Journal of Forest Research, vol. 34, no. 8, pp. 1616–1626, 2004.

- 473 [25] A. Cicione, R. Walls, Z. Sander, N. Flores, V. Narayanan, S. Stevens, and D. Rush, “The effect
474 of separation distance between informal dwellings on fire spread rates based on experimental
475 data and analytical equations,” Fire Technology, vol. 57, no. 2, pp. 873–909, 2021.
- 476 [26] V. Tihay-Felicelli, K. Meerpoel-Pietri, P. Santoni, F. Morandini, A. Pieri, and T. Barboni,
477 “Flammability study of decking sections found at the wildland–urban interface at different
478 scales,” Fire Safety Journal, p. 103838, 2023.
- 479 [27] B. Martinent, K. Meerpoel-Pietri, S. Petlitckaia, T. Barboni, V. Tihay-Felicelli, and P.-A. San-
480 toni, “Emission factors for the burning of decking slabs made of wood and thermoplastic with a
481 cone calorimeter,” Fire, vol. 6, no. 4, p. 162, 2023.
- 482 [28] S. Mouras, “Proposition pour l’adaptation des dtu bois au contexte des dom,” 2002.
- 483 [29] E. E. Smith and S. Satija, “Release rate model for developing fires,” Journal of Heat Transfer,
484 vol. 105, pp. 281–287, 1983.
- 485 [30] B. R. Toal, G. W. H. Silcock, and T. J. Shields, “An examination of piloted ignition characteris-
486 tics of cellulosic materials using the iso ignitability test,” Fire and Materials, vol. 14, pp. 97–106,
487 1989.
- 488 [31] G. W. H. Silcock and T. J. Shields, “Evaluating ignition data usgin the flux time product,” Fire
489 Safety Journal, vol. 24, pp. 75–95, 1995.
- 490 [32] T. J. Shields, G. W. Silcock, and J. J. Murray, “A protocol for analysis of time-to-ignition data
491 from bench scale tests,” Fire and Materials, vol. 18, pp. 243–254, 1994.
- 492 [33] G. B. Baker, M. J. Spearpoint, C. M. Fleischmann, and C. A. Wade, “Selecting an ignition
493 criterion methodology for use in a radiative fire spread submodel,” Fire and Materials, vol. 35,
494 pp. 367–381, 2011.